A Low-Complexity ONU Activation Scheme for TFDMA Coherent PON Systems

Xudong Wang, Yongxin Xu, Xiaokai Guan, Wenqing Jiang, Mengyue Shi, Weisheng Hu, and Lilin Yi

***Abstract*—The emergence and development of new communication services have prompted optical access systems to evolve toward higher speed rates. Coherent passive optical network (PON) based on digital subcarrier multiplexing (DSCM) has become one of the key technologies driving the evolution of optical access networks, owing to its flexible spectrum resource allocation and support for time-frequency division multiple access (TFDMA). In PON systems, a new joining optical network unit (ONU) must achieve upstream synchronization through an activation process. The activation scheme should meet the requirements of future communication services for high capacity and low latency, while imposing minimal impact on the data signal. For the TFDMA-based coherent PON architecture, we propose an innovative low-complexity and low-latency ONU activation scheme without a quiet window, which supports both ranging and frequency offset calibration. To validate the proposed scheme, experiments are conducted in a TFDMA coherent PON system with 6 × 10 GHz subcarriers. The experimental results show that the scheme can achieve a time delay estimation accuracy of 2.5 ns, while the impact of the registration signal on upstream data transmission performance is less than 0.2 dB.**

***Index Terms*—Coherent PON, time and frequency division multiple access, ONU activation, ranging.**

I. Introduction

With the advancement of technologies such as the Internet of Things (IoT), edge computing, and 5G/6G, PON systems are facing increasing demands for higher data rates, larger capacity, and lower latency [1]. To meet these demands, the evolution toward a coherent PON architecture has become a research focus. The DSCM-based TFDMA-PON enables simple and flexible point to multi-point (P2MP) connections for different users without relying on multiple wavelengths or complex optoelectronic components, making it an attractive solution for implementing coherent P2MP PONs [2]. In this architecture, new multiple access technologies and activation mechanisms need to be investigated to enable effective user differentiation and rapid upstream synchronization when multiple users simultaneously access the network.

Received 10 June 2025; revised 29 August 2025; accepted 4 September 2025. Date of publication 8 September 2025; date of current version 15 September 2025. This work was supported by the National Natural Science Foundation of China under Grant 62025503. *(Corresponding author: Lilin Yi.)*

The authors are with the State Key Laboratory of Photonics and Communications, School of Electronic Information and Electrical Engineering, Shanghai Jiao Tong University, Shanghai 200240, China (e-mail: xudongwang.7hqq@sjtu.edu.cn; xuyongxin@sjtu.edu.cn; guanxiaokai@sjtu.edu.cn; sjtujwq@sjtu.edu.cn; sjtusmy@sjtu.edu.cn; wshu@sjtu.edu.cn; lilinyi@sjtu.edu.cn).

Color versions of one or more figures in this letter are available at https://doi.org/10.1109/LPT.2025.3607514.

Digital Object Identifier 10.1109/LPT.2025.3607514

However, in conventional TDM-PON architectures, the processes of ONU discovery and ranging involve the use of quiet windows, during which the OLT must repeatedly pause upstream transmission. This results in upstream latency and interruptions to communication. For example, with a maximum differential distance of 20 km between the OLT and ONU, the delay can reach up to 200 μs [3]. To address this issue, researchers had adopted dedicated activation wavelengths (DAW), where ONUs were activated over a separate wavelength. No quiet window was allocated on the data wavelength, which effectively reduced the transmission delay caused by activation procedures [4], [5]. Other window-free activation schemes had also been developed in IM/DD-based systems, including photon ranging [6] and whisper ranging [7], which enabled registration during ongoing data transmission without quiet windows. While these studies mitigated the latency impact of quiet windows, they mainly focused on directly modulated direct detection (IM/DD) PON systems and lacked applicability to coherent architectures. [8] proposed a hybrid TFDM coherent PON with out-of-band (OOB) signaling channels for auxiliary communication. It focused on general OOB messaging, while our scheme concentrates on registration signaling using narrowband sequences placed within the guard band. For the DSCM-based coherent PON architecture, an activation scheme in the single-fiber bidirectional situation using successive interference cancellation (SIC) was proposed, which supported the simultaneous registration of multiple ONUs [9]. However, this scheme suffered from high digital signal processing (DSP) complexity. In addition, as the number of users increases, the performance of SIC degrades, and the DSP processing latency becomes non-negligible.

Therefore, this letter proposes a low-complexity ONU activation scheme for TFDMA coherent PON systems. By employing a two-fiber bidirectional architecture with a shared laser source for both upstream and downstream directions, the tasks of time delay estimation and frequency offset estimation in the upstream can be decoupled, thereby reducing the complexity of the activation process. Meanwhile, the registration signal is designed as a narrowband, low-speed signal. The new joining ONU generates the registration signal using emulated intensity modulation, placing it within the guard band between two data subcarriers. At the receiver, emulated direct detection is employed to enhance robustness against channel impairments. Finally, the signal-to-noise ratio (SNR) is improved by averaging multiple sets of received signals. To validate the proposed scheme, experiments are conducted

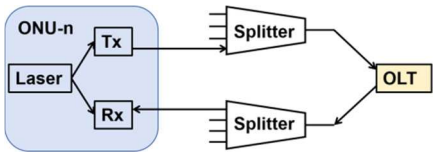

Fig. 1. Two-fiber bidirectional architecture.

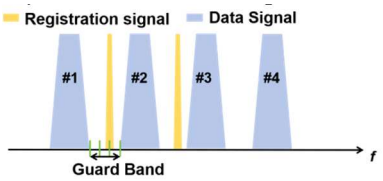

Fig. 2. Frequency domain position relationship between registration signal and data signal.

in a coherent PON system with 6 × 10 GHz subcarriers. The results demonstrate that the proposed method achieves a ranging accuracy better than 2.5 ns, while the impact of the registration signal on upstream data transmission performance is less than 0.2 dB.

II. Scheme Design

In PON systems, upstream synchronization is achieved through the activation process. The activation scheme should support ONU identification, frequency offset compensation, and time delay estimation.

In the TFDMA coherent systems, a two-fiber bidirectional architecture is considered to enable a low-complexity ONU activation scheme. By sharing a single laser source for both transmission and reception at the ONU, frequency offset compensation can be achieved through downstream synchronization. As a result, only time delay estimation is required in the upstream direction, avoiding the complexity associated with simultaneous time delay and frequency offset estimation during upstream synchronization.

To eliminate the need of the quiet window, the registration signal is placed within the guard band between data subcarriers and transmitted together with the data signal (Fig. 2). During the above process, it needs to occupy a part of the original protection band, and an additional spectral interval should be reserved between adjacent subcarriers and the registration signal to avoid interference. Therefore, for the spectrum, it may lead to a decline in spectrum utilization.

As illustrated in Fig. 2, suppose that the joining ONU is scheduled to use subcarrier #2. The ONU firstly completes frequency offset compensation in the downstream link. Then, a registration signal is transmitted and placed in the guard band between subcarrier #1 and #2.

For the design of the registration signal, the registration signal should include a unique serial number for each ONU, which can be identified by the OLT. In this experiment. However, to verify the general applicability of the proposed scheme, we randomly selected a sequence from the locally generated code set as the registration signal. If randomly selected sequences can be successfully detected in the experiment, it indicates that the proposed scheme has broad feasibility in practical applications, i.e., the actual serial number can be reliably obtained after detection. Gold sequences are adopted to construct the code set because they exhibit excellent self-correlation properties and, for the same order, provide a larger number of available sequences. The registration signals are designed as narrowband, low-speed signals, which are modulated and detected using emulated intensity modulation and detection. In this way, it can enhance robustness against channel impairments such as chromatic dispersion (CD), polarization mode dispersion (PMD), residual frequency offset, and phase noise.

At the transmitter, the Gold sequence selected by the joining ONU-i is denoted as $\boldsymbol{G}_i(n), n = 0,1,2.....N\text{-}1$. After the emulated intensity modulation, the signal can be expressed as:

$$\boldsymbol{x}_{i,X/Y}(n) = \sqrt{\boldsymbol{G}_i(n) + v_{dc}}e^{jw_i n} \tag{1}$$

where v_{dc} denotes the direct current (DC) bias and w_i represents the central modulation carrier frequency of ONU-i.

The registration signal is repeatedly sent and transmits through the channel. Here we neglect the effect of noise and assume that the channel transfer function for the PMD effect is:

$$h_{PMD} = \left[h_{xx}, h_{xy}; h_{yx}, h_{yy}\right]. \tag{2}$$

The frequency response of the chromatic dispersion (CD) in the single-mode fiber (SMF) is given:

$$H_{CD}(f) = e^{j\frac{\pi D\lambda^2 f^2 L}{c}} \tag{3}$$

where D is the dispersion coefficient, λ is the center wavelength of the optical carrier, L is the fiber distance and c is the speed of light.The time-domain transfer function of dispersion is given by:

$$h_{CD}(n) = \mathcal{F}^{-1}\left[H_{CD}(f)\right] \tag{4}$$

where $\mathcal{F}^{-1}$ is the inverse Fourier transform.

Therefore, the two polarization components received at the OLT can be expressed as:

$$\boldsymbol{r}_{i,X}(n) = \left[\left(h_{xx}\boldsymbol{x}_{i,X}(n-d)e^{j\theta} + h_{xy}\boldsymbol{x}_{i,Y}(n-d)e^{j\theta}\right) * h_{CD}\right]e^{j\Delta w_i n} \tag{5}$$

$$\boldsymbol{r}_{i,Y}(n) = \left[\left(h_{yx}\boldsymbol{x}_{i,X}(n-d)e^{j\theta} + h_{yy}\boldsymbol{x}_{i,Y}(n-d)e^{j\theta}\right) * h_{CD}\right]e^{j\Delta w_i n} \tag{6}$$

where Δw_i is the residual frequency offset of ONU-i's laser after downstream synchronization, θ is the laser phase noise, $*$ means convolution operation, and d is the time delay to be estimated.

At the receiver, the signal goes through emulated direct detection. Since the registration signals transmitted on both polarizations are the same (i.e., $\boldsymbol{x}_{i,X}(n) = \boldsymbol{x}_{i,Y}(n)$), while CD and phase noise primarily affect the phase of the signal, the impact of CD, PMD, phase noise, and residual frequency offset becomes negligible after emulated direct detection for narrowband and low-speed signal. Therefore, the received signal can be approximated as:

$$\boldsymbol{r}'_{i,X}(n) = \left|\boldsymbol{r}_{i,X}(n)\right|^2 \approx \boldsymbol{G}_i(n) + v_{dc} + n'_X \tag{7}$$

$$\boldsymbol{r}'_{i,Y}(n) = \left|\boldsymbol{r}_{i,Y}(n)\right|^2 \approx \boldsymbol{G}_i(n) + v_{dc} + n'_Y \tag{8}$$

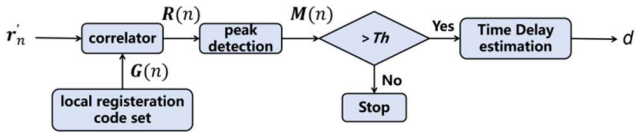

Fig. 3. Circular cross-correlation detection process of registration signal.

where the $n'_{X/Y}$ is the accumulated noise.

To minimize the impact of the registration signal on the data signal, the registration signal is transmitted at a power level significantly lower than that of the data signal. To improve the SNR of the registration signal, polarization combining is applied at the receiver, followed by multiple averaging operations to enhance the power of the effective signal:

$$\boldsymbol{r}'_i(n) = \boldsymbol{r}'_{i,X}(n) + \boldsymbol{r}'_{i,Y}(n) \tag{9}$$

The polarization-combined registration signal is circularly cross-correlated with the local sequence code set. The result of the circular cross-correlation can be expressed as:

$$\boldsymbol{R}(n) = \| \mathcal{F}^{-1}\{\mathcal{F}\{\boldsymbol{r}'(n)\}\mathcal{F}\{\boldsymbol{G}(n)\}\} \| \tag{10}$$

where $\mathcal{F}$ is the Fourier transform process, and $\mathcal{F}^{-1}$ is the inverse Fourier transform process.

After the circular cross-correlation, peak detection is then performed on the circular cross-correlation's result.

Normalized absolute peak detection (ABS) is performed as (11). If the detected peak exceeds a predefined threshold, the position of the peak is taken as the result of estimated time delay, as expressed in (12).

$$\boldsymbol{M}(n) = \frac{\boldsymbol{R}(n)}{\|\boldsymbol{r}'(n)\| \, \|\boldsymbol{G}(n)\|} \tag{11}$$

$$d = \underset{n}{argmax}\, \boldsymbol{M}(n) \tag{12}$$

III. Experimental Setup & Results

The experimental setup of our scheme is shown in Fig. 4(a). At the transmitter, 6 × 10 GBaud dual-polarization 16QAM (DP-16QAM) signals are generated to emulate the data traffic from six ONUs. The joining ONU is assigned to use the subcarrier #3, and will send the registration signal at the guard band between subcarrier #2 and #3. We select a 127-length Gold sequence as the registration signal, and modulate it using emulated intensity modulation, as shown in Fig. 4(b). Both the data and registration signals are modulated by a coherent transmitter (CDM), with an external cavity tunable laser (ECL) operating at 1550 nm, amplified by an erbium-doped fiber amplifier (EDFA), and transmitted over 20 km of standard single-mode fiber (SSMF). The power of each data signal is uniformly set to 2.02 dBm, resulting in a total EDFA output power of 9.8 dBm. The power spectrum of the data and registration signals in the X and Y polarizations are shown in Fig. 4(b), where the power of the registration signal is 15 dB lower than that of the data signal. The data signals are generated at a symbol rate of 10GBaud, with a root-raised cosine filter roll-off factor of 0.0625 and a guard bandwidth of 600 MHz.

At the receiver, a variable optical attenuator (VOA) is used to control the received power, and another 1550 nm

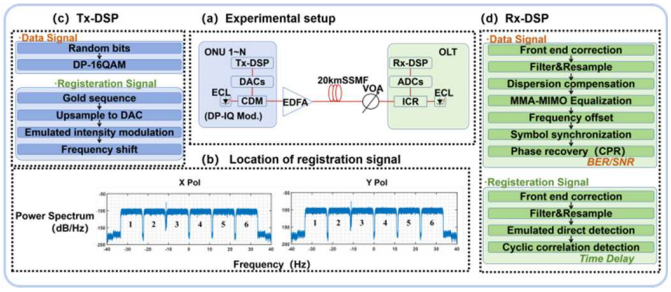

Fig. 4. (a) Experimental setup; (b) Location of registration signal; (c) Tx-DSP; (d) Rx-DSP.

ECL serves as the local oscillator (LO). Coherent detection is performed using an integrated coherent receiver (ICR), followed by analog-to-digital conversion (ADC) and offline DSP.

The receiver-side DSP flow for registration signal detection and data signal recovery is illustrated in Figs. 4(c) and 4(d). After the IQ correction and filtering, the registration and data signals are separated. The data signal is resampled to 2 samples per symbol (sps), and processed through dispersion compensation, multi-modulus algorithm (MMA)-based multiple input multiple output (MIMO) equalization, frequency offset estimation via the fourth-power method, symbol synchronization, and carrier phase recovery using a phase-locked loop (PLL). BER and SNR are then evaluated. The registration signal is similarly resampled to 2 sps, followed by emulated direct detection, polarization combining, and periodic averaging to enhance the SNR. Circular cross-correlation with the local sequence set is applied, and we use ABS to detect the peak of the correlation result. If the peak exceeds a predefined threshold, the corresponding sequence is identified and time-delay estimation is obtained.

In our experiment, to evaluate the performance of registration signal, the power difference between the registration signal and data signal is varied, and to assess the effect of residual frequency offset, the offset value is also adjusted accordingly. To minimize the error, 200 trials are conducted under each condition. At the receiver, we record the cross-correlation peak between the registration signal and the correct sequence, as well as the peaks between the registration signal and other sequences in $\boldsymbol{G}(n)$. Histogram analysis is then performed on these values, and we find that the peak distributions approximately follow a Gaussian distribution. By fitting the peak data to Gaussian distributions, two distinct distributions are obtained. The first corresponds to the correlation peaks between the registration signal and the correct sequence, labeled as "Right". The second corresponds to the peaks between the registration signal and other sequences, labeled as "Others".

Firstly, to evaluate the performance of registration signal, we change the power of registration signal and observe the variation of the detection performance. When the power of registration signal is 15, 20, 25, and 30 dB lower than that of data signal, the distributions of detection results are shown in Fig. 5(a)–(h).

The horizontal axis of (a)-(d) is the peak value υ of correlation, and the vertical axis is the probability density

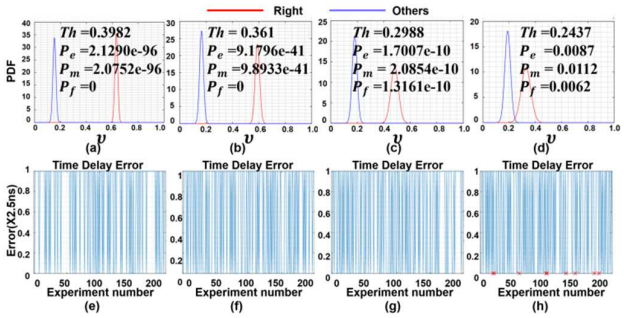

Fig. 5. With the registration signal at position 3 and power levels 15 dB, 20 dB, 25 dB, and 30 dB lower than the data signal,(a)–(d): the results of Th, P_e, P_f and P_m; (e)–(h): Time-delay estimation results.

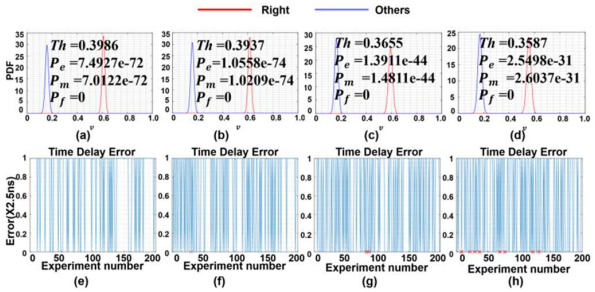

Fig. 6. With the registration signal power 15 dB lower than the data signal and residual frequency offsets of −500 MHz, −250 MHz, 250 MHz, and 500 MHz,(a)–(d): the results of Th, P_e, P_f and P_m; (e)–(h): Time-delay estimation results.

function (PDF). Th is the optimal detection threshold, P_e is false detection rate, $P_f = \int_{Th}^{\infty} f(\upsilon)d\upsilon$ is false alarm rate and $P_m = \int_0^{Th} f(\upsilon)d\upsilon$ is the missed detection rate. The P_e increases as registration signal power decreases. With $P_e < 1 \times 10^{-15}$, a Gold sequence with normalized absolute peak detection supports registration signals 20 dB lower than the data signal. For time-delay estimation, The horizontal axis of (e)-(h) is the experiment number, and the vertical axis is the time delay estimation error (×2.5ns). When the correct sequence is detected, the estimation error remains within ±1 sample (<2.5 ns) across 200 trials.

Secondly, the frequency offset of the registration signal may lead to spectral aliasing and degrade detection performance. In this scheme, the major frequency offset is compensated during the downstream synchronization process using a shared laser. Here, we evaluate the impact of residual frequency offset in the registration signal on detection performance.

As shown in Fig. 6, even with a 500 MHz residual offset, the P_e remains below $1 \times 10^1 5$, and the time-delay estimation error stays within ±2.5 ns which shows that the proposed scheme is able to successfully perform time delay estimation under residual frequency offsets within ±500MHz.

Finally, to evaluate the registration signal's impact on the data signal, the power of registration signal is set to be 15 dB lower than that of data signal. The frequency offset of registration signal is set to −500, -250, 0, 250 and 500 MHz respectively. Then, we observe the variation in BER for adjacent ONUs (#2). As shown in the Fig. 7, in our scheme, compared with w/o registration signal, the impact of registration signals with different frequency offsets remains within 0.2 dB.

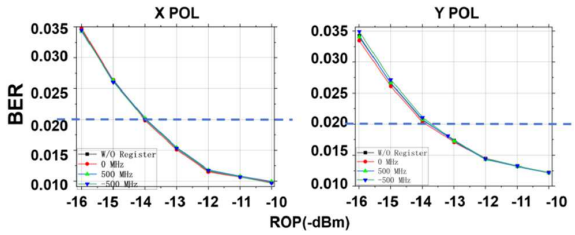

Fig. 7. The variation of BER with ROP for ONU-2 at different frequency offsets (w/o register signal, −500 MHz, MHz, 0 MHz, 500 MHz), where (a) is X polarization, and (b) is Y polarization.

IV. Conclusion

In this work, we propose a low-complexity, quiet-window-free ONU activation scheme for TFDMA coherent systems. By employing a two-fiber bidirectional architecture with a shared laser, the proposed scheme eliminates the need for frequency offset estimation during upstream activation, significantly reducing system complexity. In addition, the use of narrow-band low-speed registration signals with emulated intensity detection enhances robustness against channel impairments. Polarization combining is further applied at the receiver to improve the SNR. Experiments show the method achieves <2.5 ns ranging accuracy, tolerates ±500 MHz residual frequency offset, and causes less than 0.2 dB degradation to data signals. Accurate estimation is maintained with a 20 dB power gap between the registration and data signals. In practice, the registration signal is transmitted in burst mode, thus, burst-mode DSP (BM-DSP) is required for frame detection and synchronization. Recent work [10] has shown that such techniques are compatible with upstream coherent PONs and can be integrated into our scheme in future implementations.

References

[1] Z. Jia, H. Zhang, K. Choutagunta, and L. A. Campos, "Coherent passive optical network: Applications, technologies, and specification development [invited tutorial]," *J. Opt. Commun. Netw.*, vol. 17, no. 1, pp. A71–A86, 2025.

[2] L. A. Campos, Z. Jia, M. Xu, and H. Zhang, "Coherent optics for access from P2P to P2MP," *J. Opt. Commun. Netw.*, vol. 15, no. 3, pp. A114–A123, 2022.

[3] W. Zhang, X. Huang, and Z. Ma, "Principle and realization of low-latency 50G-PON based on special activation wavelength," *Zhongxing Commun. Technol.*, vol. 28, no. 4, pp. 58–62, 2022.

[4] J. S. Wey, Y. Luo, and T. Pfeiffer, "5G wireless transport in a PON context: An overview," *IEEE Commun. Standards Mag.*, vol. 4, no. 1, pp. 50–56, Mar. 2020.

[5] *Higher Speed Passive Optical Networks—Common Transmission Convergence Layer Specification*, document ITU-T Rec. G.9804.2, 2021.

[6] L. Bertignono, V. Ferrero, M. Valvo, and R. Gaudino, "Photon ranging for upstream ONU activation signaling in TWDM-PON," *J. Lightw. Technol.*, vol. 34, no. 8, pp. 2064–2071, Apr. 15, 2016.

[7] R. Bonk, R. Borkowski, M. Straub, H. Schmuck, and T. Pfeiffer, "Demonstration of ONU activation for in-service TDM-PON allowing uninterrupted low-latency transport links," in *Proc. Opt. Fiber Commun. Conf. Exhib. (OFC)*, San Diego, CA, USA, Mar. 2019, pp. 1–3.

[8] H. Zhang, Z. Jia, L. A. Campos, K. Choutagunta, and C. Knittle, "Hybrid TFDM coherent PON featuring adaptable capacity and out-of-band communication channels," in *Proc. Opt. Fiber Commun. Conf. (OFC)*, San Diego, CA, USA, 2024, pp. 1–3.

[9] L. Yi et al., "Joint time delay and frequency offset estimation scheme for multiple ONUs' activation in point-to-multipoint coherent PON system," *Opt. Exp.*, vol. 33, no. 9, pp. 19729–19739, 2025.

[10] J. Zhou, Z. Liu, M. Guo, H. Wang, W. Liu, and C. Yu, "Burst-mode digital signal processing for passive optical networks based on discrete multi-tone," *Opt. Exp.*, vol. 32, no. 21, p. 37148, Oct. 2024, doi: 10.1364/oe.538190.